APPENDIX A

This appendix contains a copy of the paper to be presented at the Fifth Annual Contractors' Meeting on Contaminant Control in Coal Derived Gas Streams to be held in Morgantown, West Virginia on May 7-9, 1985.

LOW TURBULENCE/HIGH EFFICIENCY CYCLONE SEPARATORS: FACILITY QUALIFICATION RESULTS

CONF-850522--4

DE91 001507

by

Richard Razgaitis [1], Darrell D. Paul [1],
Anthony A. Bioarski [1], Hans Jordan [1],
Robert S. Brodkey [2a], Melody Munson-McGee [2b]

ABSTRACT

The objective of this work is to experimentally investigate the near-wall turbulent flow-fields characteristic of cyclone separators in order to determine the influence of wall-originating turbulence on the separation of fine particles. In particular, seven turbulence suppression concepts will be evaluated with reference to a well-established baseline condition. Concepts which appear attractive will be studied and characterized in more detail.

The work accomplished to date is principally the design, construction, and qualification of two of the facilities that will be used to study the various concepts of turbulence suppression. The qualification of the primary facility, the Cyclonic Wind Tunnel (CWT), has required the development and adaptation of laser Doppler velocimetry (LDV) to perform simultaneous two-dimensional turbulence measurements in a highly swirling flow. To date, extensive LDV measurements have been made of the mean and fluctuating components of the radial and tangential velocity and the Reynolds stress, all as a function of axial (or longitudinal) position, radius, and CWT inlet velocity. These data have been obtained using three different particles: fine-droplet oil (sub-micrometer size), fine-size AC test dust (5 μm nominal size), and coarse-size pollen (20 μm nominal size). Significant differences in the radial velocity for each of these particle systems have been observed, although the radial profiles of the various turbulence parameters are similar to one another.

The initial experiments of the first turbulence suppression concept have begun. This concept consists of a rotating, transparent insert whose internal dimensions are identical to the replaced test section of the CWT. Turbulence suppression data with the three aerosols identified above are being taken as a function of rotation rate up to a maximum of 1,000 rpm.

A companion facility to the CWT is the Curvilinear Boundary Layer (CBL) apparatus. The purpose of the CBL is to provide a thick, visually-observable near-wall flow region under dynamically similar conditions to the CWT to that a physical understanding of the turbulence suppression process can be obtained.

1/ Battelle-Columbus staff; 505 King Avenue, Columbus, OH 43201
2/ Ohio State University staff; Department of Chemical Engineering, 121 Koffolt Laboratories, 140 W. 19th Avenue, Columbus, Ohio 43210
a) Professor; b) Graduate student/research assistant

The physical scales of the CWT and CBL are nearly identical, but the CBL uses water as the flow medium. To date, the design, construction, and qualification of the CBL have been accomplished. The data taken in this facility are almost exclusively based on visual recording: 35 mm still photographs, videotape, and high-speed 16 mm/cine. These data have shown two clearly distinguishable particle families: those that are moving quiescently along the wall in a helically-axial direction, and those which appear to have rapid, irregular motions in the general direction away from the wall. It is thought that additional study will reveal that the source of such irregular motions away from the wall is a Gortler vortex structure.

1.0 INTRODUCTION

Background

The need for hot-gas cleanup is well established. In order to make use of the abundant coal reserves in the U.S. in direct-cycle applications, hot effluent gas will need to be cleaned of virtually all particulate matter, especially those particles larger than about 5 μm in diameter. This is necessary in order to assure a reasonable life for the work conversion device (usually considered to be a turbine). The magnitude of this cleaning requirement remains to be established because trade-offs exist between parameters such as turbine performance and ruggedness, particle concentration and turbine life, and turbine costs and hot-gas collector costs.

The attractiveness of cyclone-type separators for this application is equally well established. Cyclones offer the following advantages:

- They are readily adaptable to hot-gas conditions.
- They can be made in a range of capacities (although the efficiency is known to decrease with larger sizes).
- They are simple, robust, and, hence, reliable, representing the most convenient means of achieving the desired collection.
- As a more or less direct consequence of the above, they are the lowest cost means of particle collection.

These qualities of cyclones are balanced by two negative aspects. The first one is the most significant. The separation efficiency of cyclones is known to decrease with decreasing particle size, especially when attempting to collect particles smaller than about 10 to 15 μm. Unfortunately, this degradation in efficiency is near, but not quite at, the threshold particle size that erodes turbine surfaces as particles smaller than about 5 μm are usually considered to be relatively benign. Cyclones of conventional design would permit far too many particles in the range of 5 to 20 μm to enter the turbine to allow reasonable operating lifetimes. A second negative aspect of cyclones is that of high pressure drop. Depending on the design conditions, the collection system pressure drop can be 5 to 10 in. of water gage (or even larger), a value which is considered to be high in comparison to that for devices such as electrostatic precipitators. For the envisioned application, which involves cleanup of a pressurized system (which will operate at several thousand inches of water pressure), this factor is perceived to be of lesser significance.

Thus, the opportunity exists to make an important contribution to the development of direct cycle systems using coal derived effluent: namely, the development of improved cyclonic systems for which the particle collection efficiency drop-off level coincides with the particle erosion deterioration threshold of approximately 5 μm diameter.

Research Objective

The research objective of this project is to 1) investigate and characterize near-wall turbulence in cyclone separators and 2) determine its influence on the separation efficiency of fine particles for both baseline and turbulence suppression conditions.

This objective will be accomplished by the use of three experimental rigs: a cyclonic wind tunnel facility (CWT), a curvilinear boundary layer facility (CBL), and a baseline cyclone facility (BCF), as illustrated in Figure 1. This report describes the design and qualification of the CWT and CBL.

2.0 THE CYCLONE WIND TUNNEL FACILITY (CWT)

The purpose of the CWT is to provide a wind tunnel that can be used as a test bed for cyclonic flows much like conventional wind tunnels have been used for rectilinear flows. The benchmark operation of this facility has been documented in a report entitled Qualification Test Plan Results for the Cyclonic Wind Tunnel Facility (Paul, Razgaitis, Boiarski, Jordan 1985).

The CWT is intended to be an analog computer representing the key features of the research hypothesis under study. The focus of the research is on the energetic turbulence structures in the near-wall region that are believed to be the cause of limited collection efficiencies for particles below approximately 20 μm. The purpose of these studies is to examine if such turbulence structures can be suppressed to a degree that will cause a significant change in the behavior of 5 to 10 μm particles. Seven different turbulence suppression techniques have been proposed for study. Four of them are wall-based techniques: a rotating wall, a porous wall, a fuzzy wall, and a grooved wall. The remaining three techniques are field-based phenomena: the use of an axial electrostatic field, an acoustic field, and a stranded field. The first phase of the experimental plan involves the screening of all seven turbulence suppression techniques to determine which concepts are the most effective at reducing the turbulence level in the near-wall region and also enhancing the particle separation potential of the cyclonic flow field. Of these, three or four will be chosen for more detailed studies to determine how the lower turbulence levels in the near-wall region affect the particle separation potentials of 5 to 10 μm particles for a range of cyclone operating conditions.

2.1 EXPERIMENTAL FACILITIES AND INSTRUMENTATION

2.1.1 Design of the CWT

The mirror-image CWT design consists of five major components: a quieting chamber, a contraction inlet, a scroll piece, the mirror-image test sections, and the exit boundary control device. These components are illustrated in Figure 2.

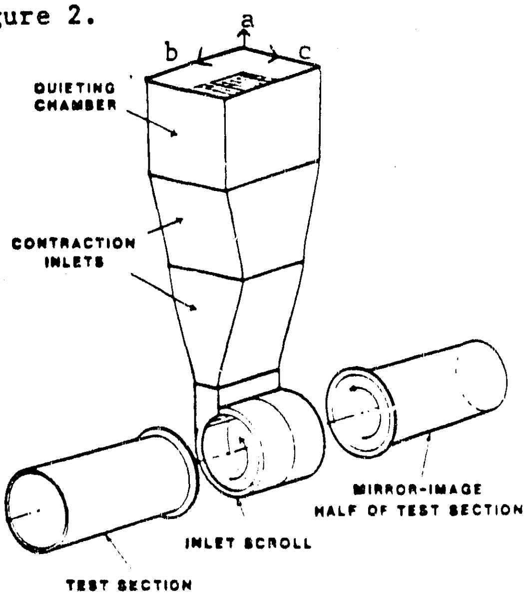

Figure 2. Cyclonic Wind Tunnel (CWT).

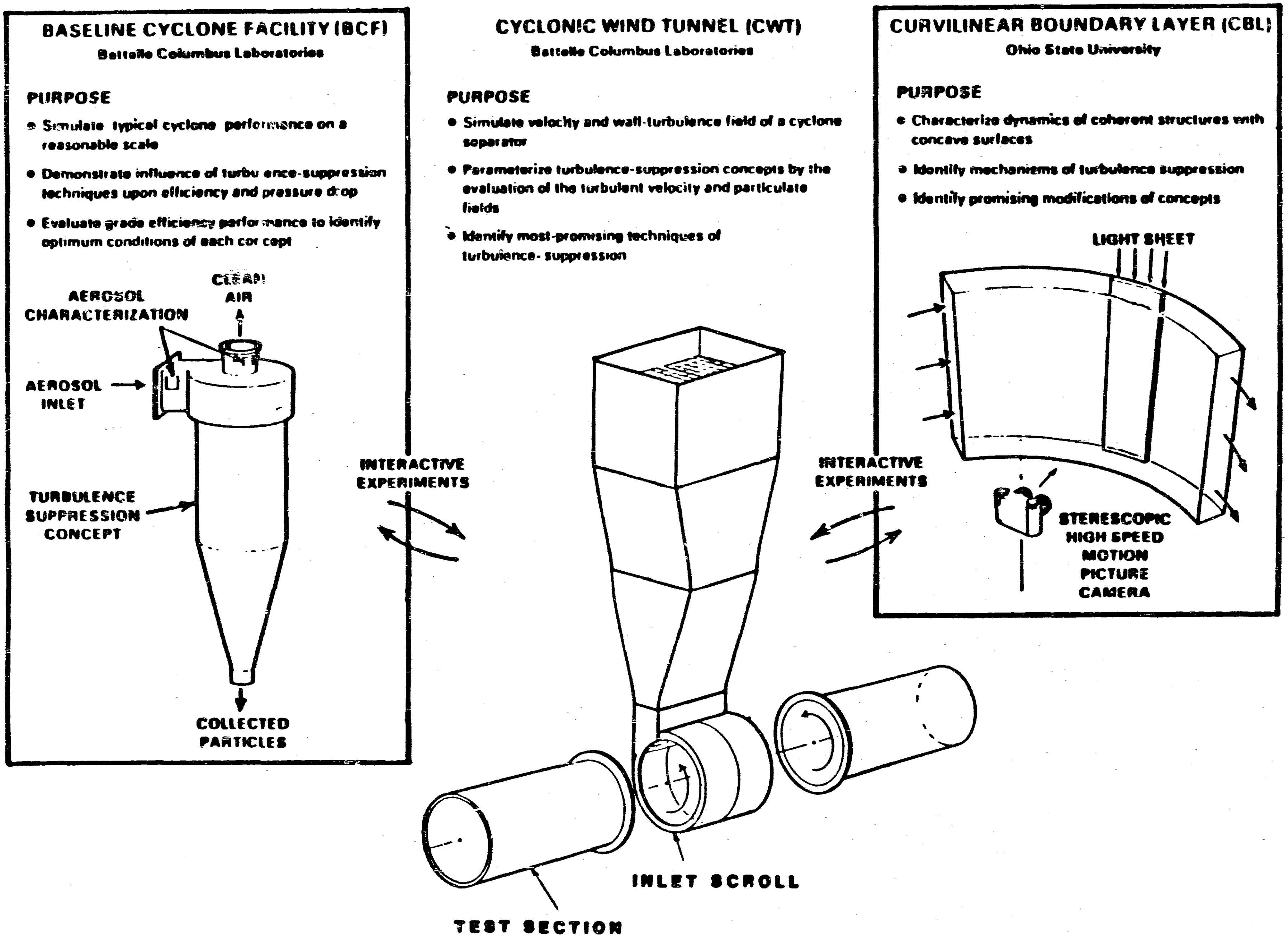

FIGURE 1. The Three-Tier Experimental Program

The quieting chamber on the cyclonic wind tunnel has been designed in accordance with the specifications used for conventional rectilinear wind tunnels (Baals and Corliss 1981; and Pope 1947). Its purpose is to eliminate any bulk swirl in the flow field induced by turns in the upstream duct work, and to produce a flow field with homogeneous turbulence. Bulk swirl is eliminated by forcing the flow through straighteners consisting of a honeycomb pattern of 16 mm tubes, each 20 diameters long. Homogeneous turbulence is produced by placing a fine mesh stainless steel screen (30 mesh spacing with an open area equal to 37 percent of the cross-sectional area) at the outlet of the flow straighteners.

Next, the flow enters a sudden contraction inlet section. A rubber coupling placed between the quieting chamber and the contraction inlet serves to isolate vibrations in the blower duct work from the rest of the wind tunnel. The purpose of the sudden contraction inlet section is to produce an extremely flat velocity profile at the inlet to the scroll piece, and to further suppress any inhomogeneities that might exist in the flow field. Two one-dimensional contractions, placed in series, allow a smooth transition from the $a_1 \times b_1$ area of the quieting chamber to the $a_2 \times b_2$ area of the scroll inlet. The first one-dimensional contraction section operates only on the "b" coordinate, changing the cross sectional area from 406 mm x 406 mm to 406 mm x 305 mm. The second one-dimensional contraction operates only on the "a" coordinate; changing the cross section area from 406 mm x 305 mm to 76 mm x 305 mm. Breaking two-dimensional contractions into two separate one-dimensional contractions is a common technique used to simplify the overall construction (Lee 1984). Each one-dimensional contraction has a cosine shape to allow a smooth transition of the flow field to the new flow area. The overall contraction ratio of 7 to 1 is in line with other wind tunnels designed to have a low turbulence inlet (Pankhurst and Holder 1953). The contraction inlet is attached to the scroll piece.

The purpose of the scroll piece is to convert the rectilinear flow field into a vortical flow field. Design specifications for conventional cyclone separator inlets have been used as a basis for the scroll inlet design. Conventional cyclones typically have tangential inlets which are one-fourth of the cyclone diameter wide and one-half the cyclone diameter in axial length (Leith and Mehta 1973). The only difference in the CWT inlet is that it has been made twice as long to accommodate the two mirror-image test sections. The rationale for the mirroring has been to avoid the formation of end-wall boundary layers in the scroll piece and their attendant disruption of the flow field.

The mirror-image test tubes form the body of the cyclonic wind tunnel and act to direct the swirling flow field along their axes. Each test section has an inside diameter of 0.292 meters and a length from the centerline of scroll inlet to the exit plane of the test sections of 1.22 m. An even split of the flow is assured because the test sections are exact mirror-images of each other with respect to the centerline of the scroll inlet. For this reason, data need only be taken in one of the test sections.

At the exit plane of each test section, a flat disk plate has been used as a boundary exit control device as shown in Figure 3. An adjustable gap exists between the flat disk plate and the exit plane of the test section. The swirling flow inside the CWT must exit radially outward through this gap. The gap tends to stabilize and preserve the vortical flow field inside the CWT. It also has the added advantage of allowing easy access for backscatter LDV measurements through the end of the CWT.

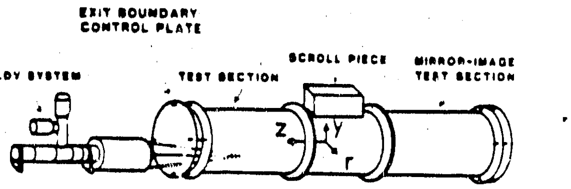

Figure 3. Schematic Diagram Of The Flat Disk Plate Used As An Exit Boundary Condition Control Device.

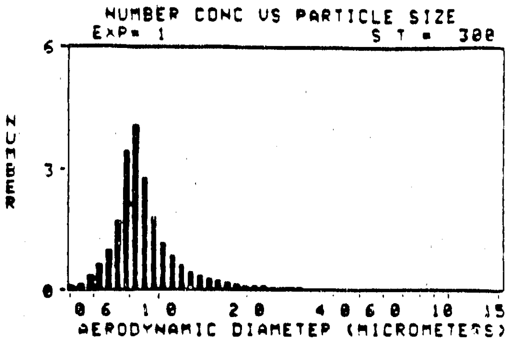

Figure 4. The Aerodynamic Particle Size Distribution Obtained For Atomized Mineral Oil Droplets Used As Tracer Particles.

2.1.2 The Aerosol System

The aerosol system consists of the equipment necessary to generate and inject seed particles of known size into the cyclonic wind tunnel (CWT). These particles are then tracked inside the CWT test sections using a laser Doppler velocimeter (LDV) to determine their behavior in cyclonic flow field.

Three types of seed particles have been chosen for the qualification tests--they will be referred to as tracers, fine particles and coarse particles. Size distributions for the tracer particles have been measured using an aerodynamic particle sizer (TSI, Inc. Model APS-33). This instrument measures the aerodynamic particle diameter, defined as "the diameter of a sphere with density 1 g/ml and with settling velocity equal to the particle in question" (Sem 1984). In addition, size distributions for the fine and coarse particles have been obtained through the analysis of micrographs (1000X magnification) of the particles taken with a scanning electron microscope. These data have been used to characterize the different types of seed particles.

The tracer particles consist of mineral oil droplets (specific gravity of 0.97) generated using a six-jet atomizer (manufactured by TSI, Inc., Model 9306). Aerodynamic particle size measurements on these particles show that they have a number average diameter of 0.85 μm (see Figure 4). The size and density of these particles are such that they should follow the turbulent fluctuations of the CWT flow field (Maxwell and Seasholtz 1977). The tracer particles are used with the LDV system to map the turbulent flow field inside the CWT test section. The tracer particles are injected into the CWT flow well upstream of the quieting chamber in order to insure a nearly uniform concentration inside the CWT.

The ideal choices for the fine and coarse particles would be monodisperse size distributions with number mean sizes of approximately 5 and 20 μm. The coarse particles (20 μm) are expected to be easily separated in a cyclonic flow field regardless of the turbulence levels at the wall. However, the fine particles (5 μm) are expected to be responsive to the turbulence fluctuations of the flow field and experience significant particle re-entrainment in the near-wall region. Turbulence suppression is expected to significantly improve the particle separation potential of the cyclonic flow field by reducing the effect of turbulent re-entrainment mechanisms. The 5 and 20 μm particles will serve as a gauge to determine how much improvement may be achieved as a function of particle size.

For the coarse particles (20 μm), short ragweed pollen obtained from Greer Laboratories (North Carolina) has been found to be ideal. Figure 5 shows a micrograph (1000X magnification) of a dispersed sample of the short ragweed pollen. Size measurements taken from the photograph show that the particles are nearly spherical in shape with an arithmetic mean size of 20.3 μm and a standard deviation of 0.5 μm. The specific gravity of the pollen is approximately 1.4 (McCrone and Delly 1973).

Pollen particles in the 5 μm size range could not be found. In order to meet the requirement of obtaining large quantities (ca. 1 Kg) of fine particles at an affordable cost, the feasibility of using several types of mechanically derived powders was examined. After spending considerable time evaluating alternatives such as metal oxide powders, glass microspheres, and sprays, it was decided to use a cut fraction of AC test dust available from a division of General Motors. The AC test dust consists of irregularly shaped silica particles (specific gravity of approximately 2.6), which have been cut down to a 5 μm size using a Majac centrifuge. Figure 6 shows a micrograph (1000X magnification) of a dispersed sample of the AC test dust. Although the sample contains a large number of particles less than 2 μm in size, these smaller particles can be optically discriminated from the large particles using the LDV system (this is explained later in the text). Thus, in analyzing the photographs only those particles greater than 2 μm in size were counted. The AC test dust had an arithmetic mean diameter, based on the best fit to the projected diameter of an equivalent sphere, of 4.8 μm and a standard deviation of 2.6 μm. However, the nonspherical shape of the particles is expected to considerably increase their drag coefficients when compared to spherical particles.

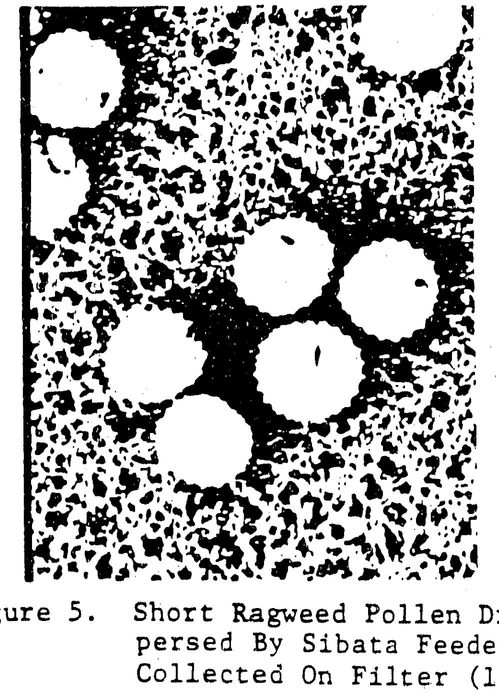

Figure 5. Short Ragweed Pollen Dispersed By Sibata Feeder and Collected On Filter (1000X Magnification SEM).

Since the 5 and 20 μm particles are large enough to experience a significant separation potential in the cyclonic flow field, a lance injector has been used to insure high concentrations of particles near the LDV measurement volume. The lance injector consists of a long, 10 mm diameter tube running along the central axis of

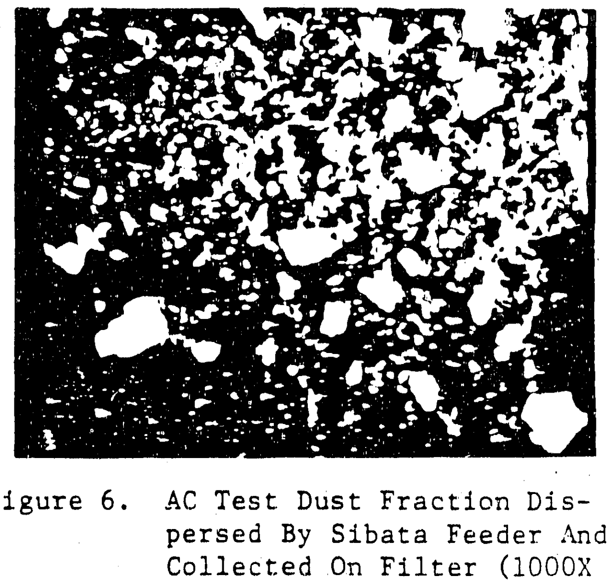

Figure 6. AC Test Dust Fraction Dispersed By Sibata Feeder And Collected On Filter (1000X Magnification, SEM)

the CWT. A Sibata microfeeder is used to disperse the powders into the lance injector. The discharge end of the lance injector is positioned upstream of where LDV measurements are to be taken. Particles injected along the centerline spiral toward the wall due to the large centrifugal force field inside the CWT. The particle response times of the 5 and 20 μm particles are on the order of 0.1 and 1.0 ms, respectively. These particles do not "remember" how they were injected once they travel beyond a short distance from the CWT centerline. Therefore, by restricting our LDV measurements to the near-wall region the location of the lance injector should not affect the precision of the results.

2.1.3 Laser Doppler Velocimetry System

All measurements of the turbulent flow field inside the cyclonic wind tunnel have been performed using a laser Doppler velocimeter (LDV). The LDV measures the Doppler frequency of light scattered from seed particles in the flow field to determine the velocity of the particle. This nonintrusive measurement technique is particularly well-suited for measuring the radial velocity component of the cyclonic flow field and for tracking the individual particle motions inside the CWT. Insertion probes, such as hot wire anemometers or pitot probes, are incapable of adequately performing either one of the above functions. Therefore, the LDV is the key tool needed to ensure the success of this research program.

Figure 7 shows the complete three beam, two color LDV system (manufactured by TSI, Inc.) that has been used to obtain the simultaneous point-wise measurements of tangential and radial velocities inside the cyclonic wind tunnel. The LDV system uses a 2 watt argon ion laser (Coherent Model CR-2) operating with all lines, and dichroic filter separation to obtain the blue (488 nm) and green (514.5 nm) beams

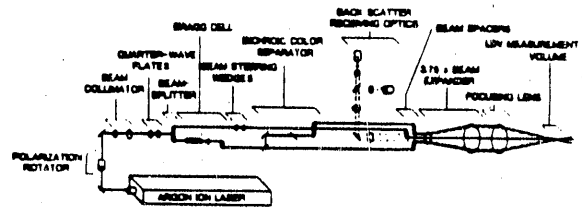

Figure 7. Schematic Diagram of Laser Doppler Velocimeter Showing The Arrangment Of The Components.

needed for two channel operation. The blue light is used to measure the tangential velocity while the green light is used to measure the radial velocity of the flow field. Both the blue and green beam channels employ frequency shifting of 10 MHz and 5 MHz, respectively, to determine the direction of fluid motion.

The LDV system has been set up to operate in a backscatter mode so that only one optical window is needed to obtain velocity measurements. A 3.75X beam expander with a 152 mm diameter lens has been employed to greatly enhance the signal-to-noise ratio of the system. Scattered light from the LDV measurement volume is collected through the same focusing lens used to transmit the beams, thereby eliminating the need to align the receiving optics. A dichroic color separator in the receiving optics train permits discrimination between the scattered light coming from the green and blue beams.

Each photomultiplier tube/amplifier system has a frequency response of 200 MHz. The output signal of the photomultiplier tubes is analyzed using counter processors--one for the blue beam data and the other for the green beam data. For the data reported here, the Doppler signals were validated by the counter processors using the most-stringent criteria, 16 cycles per burst, with a comparison ratio (a measure of the consistency of the time interval between cycles) of less than

1 percent. The output of the counter processors is fed to a multichannel interface. Data will only be accepted from the two counter processors if the output signals reach the interface within a coincidence window of 10 μs. This insures the Doppler bursts recorded in both channels were produced by the same particle traversing the measurement volume. An analog-to-digital converter is then used to transmit the data to an Apple II microcomputer.

The microcomputer collects the data from approximately 2000 individual particles traversing the measurement volume before proceeding with the statistical analysis. At each measurement point, the mean tangential velocity $\langle U_\theta \rangle$, the tangential turbulence intensity U_θ', the mean radial velocity $\langle U_r' \rangle$, the radial turbulence intensity U_r, and the Reynolds stress component $\langle U_r U_\theta \rangle$ are calculated. These data may be stored on a floppy disk and/or a hard copy printed.

The optical components of the LDV system have been mounted on an optics table that has the capability of traversing in the r-z (horizontal) plane. The axial position, z, is adjusted by rolling the table on a rail mount to the desired location. A programmable controller connected to a stepper motor is used to drive the optics table to any radial position within the cyclonic wind tunnel. The Apple II microcomputer keeps track of the position of the optics table, and prints this information along with the rest of the LDV output data. In this manner, rapid data taking is possible once the LDV system is aligned inside the CWT.

2.2 THE BASELINE CONDITIONS

The qualification test plan for the cyclonic wind tunnel (CWT) facility has been used to establish a set of baseline conditions (Paul et al 1985). The baseline conditions define the turbulence parameters and particle interaction behavior inside the CWT without any turbulence suppression inserts. These baseline conditions will be the standard used to judge the effectiveness of each turbulence suppression concept. This section summarizes the important findings of the qualification test plan and defines the set of baseline conditions.

Mapping studies of the CWT flow field have shown that the turbulence parameters of interest remain nearly constant in the axial segment bounded by $2.12 < z^* < 3.87$, where z^* is the axial distance from the mid-plane of the scroll inlet divided by the inside diameter of the CWT. For our previous studies on the interactions of fine and coarse particles with the cyclonic flow field, we have chosen the test section to be at an axial distance of $z^* = 3.66$ from the mid-plane of the scroll inlet. At this location, LDV measurements were taken in the near-wall region, i.e., $0.48 < r^* < 0.95$.

Tracer particles consisting of mineral oil droplets ($\langle D_p \rangle = 0.85$ μm, $\sigma_p = 1.52$ μm, $\rho = 0.97$ g/ml) have been used to map the flow field parameters. For the particle interaction studies, we have chosen AC test dust ($\langle D_p \rangle = 4.8$ μm, $\sigma_p = 2.6$ μm, $\rho = 2.6$ g/ml), hereafter referred to as the fine particles, and short ragweed pollen ($\langle D_p \rangle = 20$ μm, $\sigma_p = 0.5$ μm, $\rho = 1.4$ g/ml), hereafter referred to as the coarse particles. The fine (5 μm) and coarse (20 μm) particles will allow us to obtain a set of baseline test conditions as a function of particle size. In later tests involving turbulence suppression, it is expected that the separation potential of the fine particles will be significantly enhanced by turbulence suppression; whereas the coarse particles should only be slightly affected since they already have high separation potentials.

As the particles pass through the measurement volume of the LDV, their tangential and radial velocities and turbulence intensities are measured along with the corresponding Reynolds stress component. Figure 8 shows the normalized mean tangential velocity profiles, ($\langle U_\theta \rangle / U_O$) for the tracer particles, the fine particles, and the coarse particles. These data have been normalized using the scroll inlet velocity, U_O, calculated from the measured total CWT flow rate. The lines drawn on the graphs are the best fits to the tracer particle data. The data for the fine and coarse particles show that these particles have slightly lower mean tangential velocities for $r^* = (r/R)$ values less than 0.75. The reason for this is probably due to the velocity lag effect experienced by the particles as they drift radially outward along a velocity gradient, and also due to the Coriolis force which acts to retard tangential motion of particles with significant radial drift velocities. For $r^* = (r/R)$ values greater than 0.75, the negative velocity gradient is expected to give tangential velocities for the fines slightly greater than the tracers, again because of the velocity lag effect, but this phenomenon is balanced by the Coriolis force that still tends to retard the tangential motion. The net effect is that the mean tangential velocities for $0.75 < r^* < 0.95$ are nearly identical for the tracers and the other particles in this region.

Figure 9 shows the normalized tangential turbulence intensities, (U_θ'/U_O), for the tracer particles and the samples of fine and coarse particles. The solid lines drawn on the graphs are the best curve fits to the tracer particle data. The small discrepancies between the particles and the tracers may again be caused by a lag effect experienced by the larger particles as they drift radially outward through regions of turbulence intensity gradients.

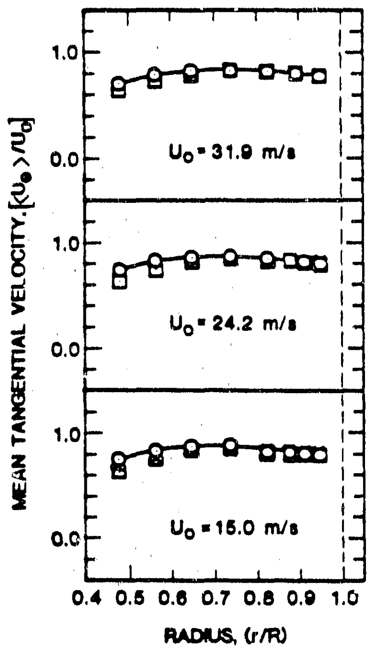

Figure 8. The Mean Tangential Velocity Profiles For Particles With Diameters of: ○ 0.85 μm; ✧ 5.0 μm; And □ 20 μm. (The Solid Line Represents The Best Curve Fit To The Tracer Particle Data.)

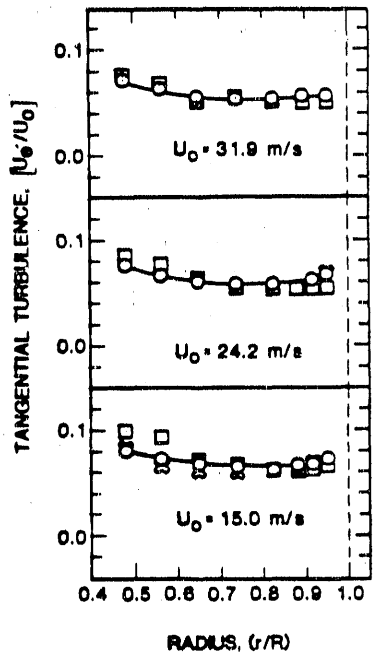

Figure 9. The Tangential Turbulence Intensity Profiles For Particules With Diameters Of: ○ 0.85 μm; ✧ 5.0 μm; And □ 20 μm. (The Solid Line Represents The Best Curve Fit To The Tracer Particle Data.)

Figure 10 shows the normalized mean radial velocity ($\langle U_r \rangle / U_0$) profiles for the tracer particles and the fine and coarse particles. In this figure, positive radial velocities are caused by particles moving toward the wall, and, conversely, negative radial velocities are caused by particles moving away from the wall. The tracer particles are small enough that they do not experience a significant centrifugal force and therefore should follow the flow field. On the other hand, the fine and coarse particles have densities and sizes which are large enough to cause these particles to experience a significant centrifugal force. This effect shows up for these particles as a shift toward the positive direction of the radial velocity profile. The difference between the measured radial velocity of the particles and that of the tracers is defined as the particle drift velocity, $\langle U_p \rangle$.

Figure 11 shows the normalized particle drift velocity ($\langle U_p \rangle / U_0$) profiles for the fine and coarse particles. The particle drift velocities increase with the scroll inlet velocity. This is expected because increases in the scroll inlet velocity translate directly into increases in the tangential velocity profile (see Figure 8) and hence the centrifugal force. The fine particles experience a particle drift velocity which is much lower than that of the coarse particles due primarily to the differences in size.

Figure 12 shows the normalized radial turbulence intensity (U_r'/U_0) profiles for the tracer, fine and coarse particles. The solid lines drawn on the graphs are the best curve fits to the tracer particle data. Radial turbulence intensity profiles for the particles show slightly lower values than the tracer data. This effect can be attributed, in part, to the longer

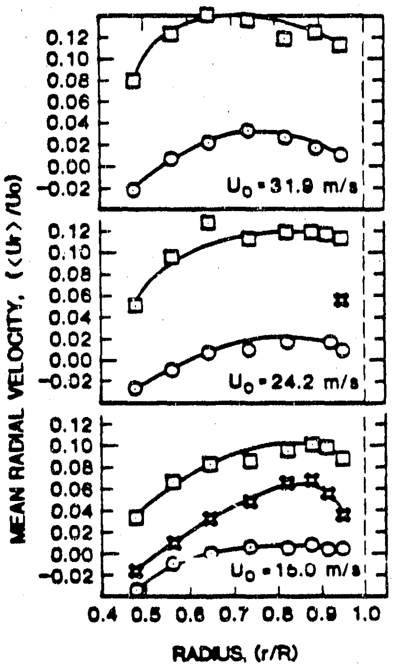

Figure 10. The Mean Radial Velocity Profiles For Particles With Diameters Of: ○ 0.85 μm; ✕ 5.0 μm; And □ 20 μm. Positive Values Signify Movement Toward The CWT Wall.

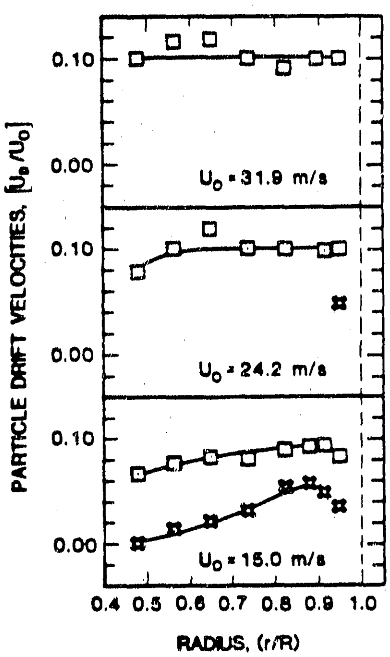

Figure 11. The Mean Particle Drift Velocity Profiles For Particules With Daimeters Of: ✕ 5.0 μm; And □ 20 μm. Positive Values Signify Movement Toward The CWT Wall.

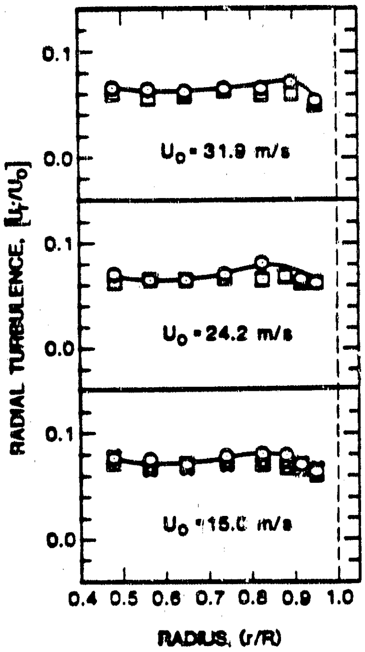

Figure 12. The Radial Turbulence Intensity Profiles For Particles With Diameters Of: ◯0.85 m; ✲5 m; And □20 m. (The Solid Line Represents The Best Curve Fit To The Tracer Particle Data.)

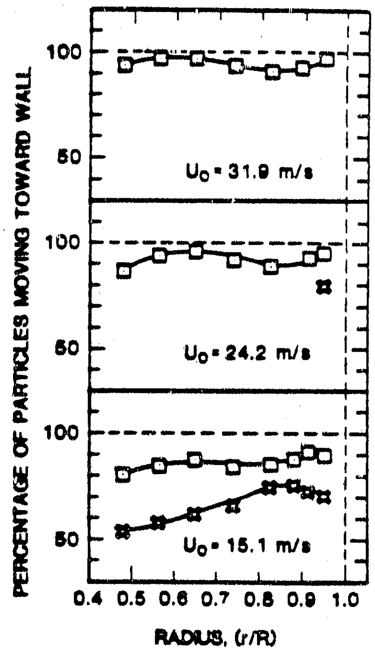

Figure 13. The Percentage Of Particles Moving Toward The CWT Wall As A Function Of Particle Size, Scroll Inlet Velocity, And Radial Position (✲5 μm and □20 μm Particles).

response times of the particles, but the differences are insignificant.

For a monodisperse aerosol with a fast response time, such as the coarse particles (σ_p = 0.5 μm), one would expect nearly identical radial turbulence intensities when compared to the tracers, as was observed. However, for a polydisperse aerosol with a fast response time, such as the fine particles (σ_p = 2.6 μm), one would expect a broadening of the radial turbulence intensity due to variations in the particle drift velocities with particle size. This effect was minimized with the fine particles because the laser Doppler velocimeter optically discriminates between particle sizes outside of its optimum range.

The optimum particle size range of an LDV system is a complex function of the LDV fringe spacing, the light scattering characteristics of the seed particles, and the electronic signal processing. For our LDV system, the optimum particle size has been estimated to be somewhere between 4 and 6 μm. Our LDV system will preferentially measure the velocities of particles in this size range even though particles of other sizes may be present. This probably explains why we did not see a broadening of radial turbulence intensity profiles for the fine particles.

Figure 13 shows the percentage of particles moving toward the CWT wall as a function of particle size, scroll inlet velocity, and radial position. For 20 μm particles, as the scroll inlet velocity increases and hence the magnitude of the centrifugal force field increases, the percentage of particles moving toward the wall increases as would be expected. For 5 μm particles, only one complete profile was obtained at U_0 = 15.0 m/s before one of our counter processors failed. (The unit has been shipped back to the factory for repair and the remaining two profiles will be measured upon its return.) Nonetheless, the 5 μm particles show significantly fewer particles moving toward the CWT wall. This is a direct result of the 5 μm particles having drift velocities that are less than the rms radial turbulence levels inside the CWT.

Consequently, if the radial turbulence level can be suppressed, then the percentage of 5 μm particles moving toward the wall can be improved. These data will provide the standard for judging the performance of various turbulence suppression concepts.

Lastly, Figure 14 shows the normalized Reynolds stress component profiles for the tracer, fine, and coarse particles. The solid lines drawn on these graphs correspond to the best curve fits to the tracer particles. Although there is a large scatter in the experimental data, the Reynolds stress component shows a peak value near the wall. Large positive values of the Reynolds stress component correspond to the production of turbulence. Positive values of the Reynolds stress component for the fines correspond to a positive correlation between the radial drift velocities of the particles toward the wall and the tangential velocity. This would be expected to occur for the fine or coarse particles since the centrifugal force on the particle is a function of the tangential velocity. However, the large scatter in the experimental data makes interpretation difficult. Presently, a method is

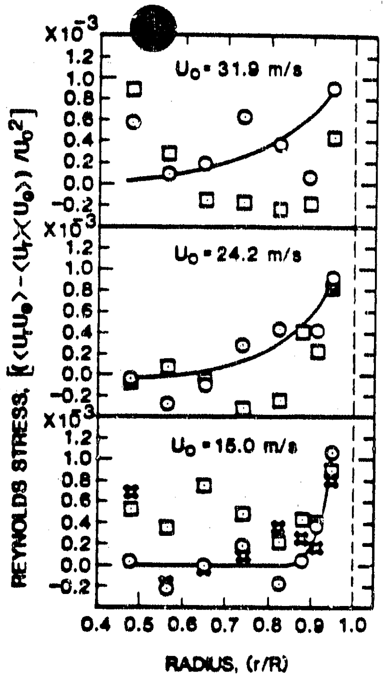

Figure 14. The Reynolds Stress Component Profiles For Particles With Diameters Of: ○ 0.85 μm; ✕ 5.0 μm; AND □ 20 μm. (The Soild Line Represents The Best Curve Fit To The Tracer Particle Data.)

being investigated to statistically discriminate against points that are more than three standard deviations from the mean of either the radial or tangential velocity components. This should eliminate the large errors associated with the measurement of the Reynolds stress component.

The above data define the set of baseline conditions for the turbulence parameters and particle interaction behavior in the cyclonic wind tunnel. All of the experimental results involving turbulence suppression inserts will be interpreted relative to these baseline conditions. The next phase of the program involves testing the seven different turbulence suppression concepts.

3.0 THE CURVILINEAR BOUNDARY LAYER FACILITY (CBL)

The Curvilinear Boundary Layer Facility (CBL) located at The Ohio

State University is another part of the Low Turbulence/High Efficiency Cyclone Separator Project. The purpose of this facility is to produce a boundary layer similar to those found in cyclonic flows. Study of the small scale motions in this boundary layer should provide insight into the limited efficiency found in cyclone separators at particle sizes below 20 μm. The final result of this work will be a comparison of unmodified CBL operation with operation employing several turbulence suppression techniques.

The main focus of work on the CBL so far has been on qualifying the facility to establish unmodified flow characteristics. Three areas were targeted for study to determine the baseline flow patterns.

The first area studied was the overall gross flow patterns of the entire CBL, utilizing video techniques. Figure 15 shows a schematic diagram of the two distinctive regions which were observed: 1) a chaotic core region with a distinct downward flow, and 2) a wall region that showed strong upwards motion in the expected manner.

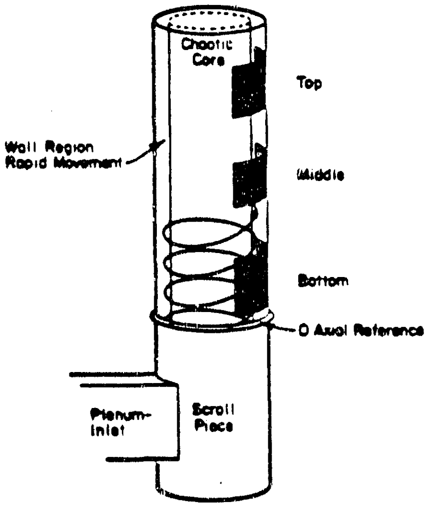

Figure 15. Schematic Diagram Of The Flow Patterns Inside The Curvilinear Boundary Layer Facility.

The second area studied was a quantitative analysis of the region near the wall. This focused on correlating the free-stream velocity of the wall region region with inlet flow rate and axial position. Velocities were calculated as a small ensemble averages for the free-stream, vertical, and tangential velocities.

The third effort examined the small scale motions in the wall region for the unmodified flow. Qualitative observations were made of flow very near the wall at different axial locations and inlet flow rates. Small scale motions were observed at all conditions studied. These motions were exhibited by particles traveling very close to the wall. Typically, a particle following a path concentric to the wall got caught up in a sinusoidal motion with an amplitude of approximately 3 mm. This motion usually continued for several centimeters, after which the particle returned to the faster moving flow.

With the baseline operating characteristics established, future work will focus on the study of turbulence suppression techniques aimed at reducing the small scale motions in the wall region.

4.0 THE BASELINE CYCLONE FACILITY (BCF)

The third and final apparatus that will be used in this program is a full-size cyclone separator. The cyclone will be operated using redispersed fly-ash in both baseline and various turbulence suppression modes. The purpose of these studies will be to demonstrate the effects of turbulence suppression in an actual cyclone at a 3-foot diameter scale.

The outcome of these data will then be used in a systems integration study to assess the practicality and system implications of the leading turbulence suppression candidates.

5.0 SUMMARY AND CONCLUSIONS

The cyclonic wind tunnel facility has been shown to generate a turbulent flow field that is representative of the near wall region of cyclone separators.

A set of baseline conditions have been obtained using this facility. These measurements will provide the basis for judging the performance of seven different turbulence suppression concepts. If the turbulence suppression concepts are effective, the lower turbulence levels and reduced bursting rates should cause a decrease in particle reentrainment near the wall. This will show up in our measurements as an increase in the mean particle drift velocities toward the wall, and also as a higher fraction of particles moving toward the wall. The turbulence suppression concepts that show the most promise will then be tested in an actual cyclone to determine the net increase in particle collection efficiency as a function of particle size.

The curvilinear boundary layer facility has been used to provide flow visualization studies of the coherent structures present in the turbulent boundary layer of cyclonic flows.

The phase of work involving the baseline cyclone facility has not yet begun.

6.0 NOMENCLATURE

English

a	Width of cross sectional flow area of contraction inlet
A	Cross sectional area
b	Length in the z direction of the cross sectional flow area of the contraction inlet
D	Diameter of particle
Q	Volumetric flow rate of air
r	Coordinate direction
R	Radius of curvature of the cyclonic wind tunnel
U	Velocity
y	Coordinate direction
z	Coordinate direction

Greek

ρ	Density
σ	Standard deviation

Subscripts

D	Particle drift velocity
p	Particle
r	Radial component
y	y component
z	z component
θ	Tangential component
0	Scroll inlet
1,2	Section numbers

Superscripts

$'$	Fluctuating component
*	Normalized with respect to the radius of curvature of the cyclonic wind tunnel

Other Symbols

$\langle\ \rangle$	Average of quantity enclosed

7.0 REFERENCES

Baals, D.D. and W.R. Corliss, Wind Tunnels of NASA, National Aeronautics and Space Administration, NASA SP-400, Washington, DC, (1981).

Lee, J., Director aerospace research, OSU, private communication, (1984).

Leith, D. and D. Mehta, "Cyclone Performance and Design", Atmospheric Environment, Vol. 7, pp. 527-549, (1973).

Maxwell, B.R., and R.G. Seasholtz, "Velocity Lag of Solid Particles in Oscillating Gases Passing Through Shcok Waves," NASA TN D7490, (1974); as quoted by Riethmuller, (1977).

McCrone, W.C. and J.G. Delly, The Paticle Atlas, Ann Arbor Science, (1973).

Pankhurst, R.C. and D.W. Holder, Wind-Tunnel Technique, Sir Pitman & Sons, London, (1953).

Paul, D.D., R. Razgaitis, A.A. Boiarski, and H. Jordan, "The Qualification Test Plan Results for the Cyclonic Wind Tunnel Facility," Topical Report submitted to DOE Morgantown Energy Technology Center, Contract No. DE-AC21-83MC20108, (February 22, 1985).

Pope, A. Wind Tunnel Testing, John Wiley & Sons, New York (1947).

Sem, G.J., "Aerodynamic Particle Size: Why is it Important?", TSI Quarterly, Vol. 10, No. 3, pp. 3-12, (1984).

END

DATE FILMED

11 / 09 / 90